

# Adaptive Refinement for $hp$ -version Trefftz Discontinuous Galerkin Methods for the Homogeneous Helmholtz Problem

Scott Congreve

Joint work with

Ilaria Perugia (Universität Wien)  
Paul Houston (University of Nottingham)

NA Seminar, University of Bath, April 12th 2019

## 1 Introduction

- Helmholtz Equation
- Continuous Galerkin FEM
- Problems with FEM for Helmholtz

## 2 Trefftz DG (TDGFEM) for Helmholtz

- Trefftz FEM Spaces
- Plane Waves
- Comparison to Polynomial DG
- Formulation

## 3 Adaptive Refinement

- Plane Wave Direction Refinement
- A posteriori Error Estimates
- $hp$ -adaptive Refinement
- Numerics

# Section 1

## Introduction

# Helmholtz Equation

Let  $\Omega \subset \mathbb{R}^d$ ,  $d = 2, 3$  be a bounded polygonal/polyhedral domain. We seek  $u : \Omega \mapsto \mathbb{C}$  such that

$$\begin{aligned} -\Delta u - k^2 u &= 0 && \text{in } \Omega, \\ u &= 0 && \text{on } \Gamma_D, && \text{(sound-soft scattering)} \\ \nabla u \cdot \mathbf{n} &= 0 && \text{on } \Gamma_N, && \text{(sound-hard scattering)} \\ \nabla u \cdot \mathbf{n} + ik\vartheta u &= g_R && \text{on } \Gamma_R, \end{aligned}$$

where

$$k = \frac{\omega L}{c}$$

is the wavenumber ( $\omega$  is the frequency of the wave,  $L$  is the measure of the domain, and  $c$  is the speed of sound in the material). Wavenumber is related to the wave length

$$\lambda = \frac{2\pi}{k}.$$

Multiplying by a test function and integrating by parts gives the **weak formulation**: Find  $u \in H^1(\Omega)$  such that

$$\int_{\Omega} (\nabla u \cdot \nabla \bar{v} - k^2 u \bar{v}) \, dx + \int_{\Gamma_R} iku \cdot \mathbf{n} \bar{v} \, ds = \int_{\Gamma_R} g_R \cdot \mathbf{n} \bar{v} \, ds$$

for all  $v \in H^1(\Omega)$ .

Well-posedness: [Melenk, 1995]

# FEM for Helmholtz

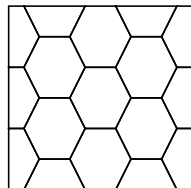
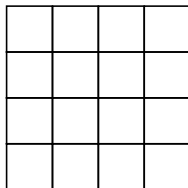
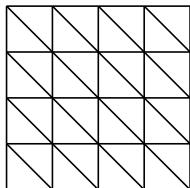
Multiplying by a test function and integrating by parts gives the **weak formulation**: Find  $u \in H^1(\Omega)$  such that

$$\int_{\Omega} (\nabla u \cdot \nabla \bar{v} - k^2 u \bar{v}) \, dx + \int_{\Gamma_R} iku \cdot \mathbf{n} \bar{v} \, ds = \int_{\Gamma_R} g_R \cdot \mathbf{n} \bar{v} \, ds$$

for all  $v \in H^1(\Omega)$ .

Well-posedness: [Melenk, 1995]

We want to search for a solution in a finite dimensional subspace of  $H^1(\Omega)$ . To that end we subdivide the domain  $\Omega$  into a mesh  $\mathcal{T}_h$  of non-overlapping elements  $K$ , where each element has a size  $h_K$ .



We can denote by  $\mathcal{F}_h^I$ ,  $\mathcal{F}_h^R$  and  $\mathcal{F}_h^D$  all interior, Robin boundary, and Dirichlet boundary edges/faces, respectively.

We can now define a subspace on this mesh:

$$V_q^{CG}(\mathcal{T}_h) := \{v \in H^1(\Omega) : v|_K \in \mathcal{S}_q(K), K \in \mathcal{T}_h\} \subset H^1(\Omega),$$

then we can define the **continuous Galerkin finite element method** (CGFEM):

Find  $u_h \in V_q^{CG}(\mathcal{T}_h)$  such that

$$\int_{\Omega} (\nabla u \cdot \nabla \bar{v} - k^2 u \bar{v}) \, dx + \int_{\Gamma_R} iku \cdot \mathbf{n} \bar{v} \, ds = \int_{\Gamma_R} g_R \cdot \mathbf{n} \bar{v} \, ds$$

for all  $v_h \in V_q^{CG}(\mathcal{T}_h)$ .

We can now define a subspace on this mesh:

$$V_q^{CG}(\mathcal{T}_h) := \{v \in H^1(\Omega) : v|_K \in \mathcal{S}_q(K), K \in \mathcal{T}_h\} \subset H^1(\Omega),$$

then we can define the **continuous Galerkin finite element method** (CGFEM):

Find  $u_h \in V_q^{CG}(\mathcal{T}_h)$  such that

$$\int_{\Omega} (\nabla u \cdot \nabla \bar{v} - k^2 u \bar{v}) \, dx + \int_{\Gamma_R} iku \cdot \mathbf{n} \bar{v} \, ds = \int_{\Gamma_R} g_R \cdot \mathbf{n} \bar{v} \, ds$$

for all  $v_h \in V_q^{CG}(\mathcal{T}_h)$ .

We can also define a **discontinuous Galerkin finite element method** (DGFEM), where the space of functions is **discontinuous** over element boundaries:

$$V_q^{DG}(\mathcal{T}_h) := \{v \in L^2(\Omega) : v|_K \in \mathcal{S}_{q_K}(K), K \in \mathcal{T}_h\} \not\subset H^1(\Omega).$$

Here we integrate by parts **elementwise** and introduce fluxes on the edges/faces,



Problems with FEM:

- Number of *degrees of freedom* required to obtain given accuracy increases with wave number  $k$ .
- Error: best approximation + phase lag:

$$\|\nabla_h(u - u_h)\|_{L^2(\Omega)} \lesssim (kh)^p + k(kh)^{2p}$$

convergence like the best approximation when  $k(kh)^{2p} \lesssim (kh)^p$ , i.e.

$$h \lesssim k^{-1-1/p} \quad (\text{resolution condition})$$

## Section 2

# Trefftz DG (TDGFEM) for Helmholtz

Polynomial DG Finite Element Spaces: DGFEM uses polynomial basis functions defined on a reference element  $\hat{K}$ :

$$V_q^{DG}(\mathcal{T}_h) := \{v \in L^2(\Omega) : v|_K \circ F_K \in \mathcal{S}_{q_K}(\hat{K}), K \in \mathcal{T}_h\}.$$

**Polynomial DG Finite Element Spaces:** DGFEM uses polynomial basis functions defined on a reference element  $\widehat{K}$ :

$$V_q^{DG}(\mathcal{T}_h) := \{v \in L^2(\Omega) : v|_K \circ F_K \in \mathcal{S}_{q_K}(\widehat{K}), K \in \mathcal{T}_h\}.$$

**Trefftz Finite Element Space:** Use basis functions defined element-wise based on functions in the kernel of the Helmholtz operator.

First define the local Trefftz spaces

$$T(K) := \{v|_K : -\Delta u - k^2 u = 0\}$$

and let

$$T(\mathcal{T}_h) := \{v \in L^2(\Omega) : v|_K \in T(K), K \in \mathcal{T}_h\}.$$

# Trefftz FEM Spaces

**Polynomial DG Finite Element Spaces:** DGFEM uses polynomial basis functions defined on a reference element  $\hat{K}$ :

$$V_q^{DG}(\mathcal{T}_h) := \{v \in L^2(\Omega) : v|_K \circ F_K \in \mathcal{S}_{q_K}(\hat{K}), K \in \mathcal{T}_h\}.$$

**Trefftz Finite Element Space:** Use basis functions defined element-wise based on functions in the kernel of the Helmholtz operator.

First define the local Trefftz spaces

$$T(K) := \{v|_K : -\Delta u - k^2 u = 0\}$$

and let

$$T(\mathcal{T}_h) := \{v \in L^2(\Omega) : v|_K \in T(K), K \in \mathcal{T}_h\}.$$

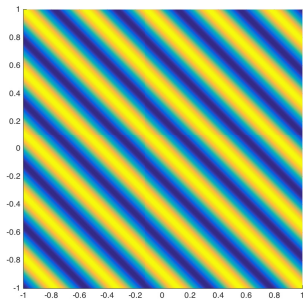
We let  $V_p(K) \subset T(K)$  be a finite dimensional local space; then, the **Trefftz FE Space** is given by

$$V_p(\mathcal{T}_h) := \{v \in T(\mathcal{T}_h) : v|_K \in V_p(K), K \in \mathcal{T}_h\}.$$

# Trefftz FE Spaces

For Helmholtz we can use the following basis functions:

Plane Waves:  $\mathbf{x} \mapsto e^{i\mathbf{k}\mathbf{d}\cdot\mathbf{x}}$ , where  $\mathbf{d}$  is a direction vector.

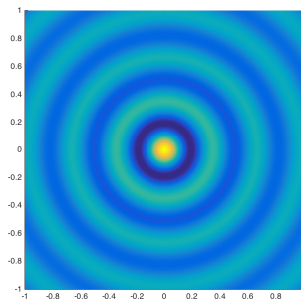
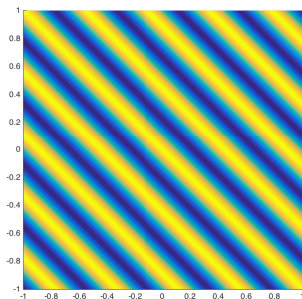


# Trefftz FE Spaces

For Helmholtz we can use the following basis functions:

**Plane Waves:**  $\mathbf{x} \mapsto e^{i\mathbf{k}\mathbf{d}\cdot\mathbf{x}}$ , where  $\mathbf{d}$  is a direction vector.

**Circular/Spherical Waves**  $\mathbf{x} \mapsto \mathcal{J}_\ell(k|\mathbf{x}|)e^{i\ell\theta}$  (in 2D), where  $\theta$  is the angle of  $\mathbf{x}$  in polar coordinates,  $\ell \in \mathbb{Z}$ , and  $\mathcal{J}_\ell$  is the Bessel function of the first kind of order  $\ell$ .



# Plane Waves

$$V_p(K) = \left\{ v : v(\mathbf{x}) = \sum_{\ell=1}^{p_K} \alpha_\ell e^{ik\mathbf{d}_\ell \cdot (\mathbf{x} - \mathbf{x}_K)}, \alpha_\ell \in \mathbb{C} \right\}$$

where  $p_K$  is the number of *degrees of freedom* for the element  $K$ ,  $\mathbf{d}_\ell$ ,  $\ell = 1, \dots, p_K$  are  $p_K$  (roughly) **evenly spaced** unit direction vectors, and  $\mathbf{x}_K$  is the centre of the element.



# Plane Waves

$$V_p(K) = \left\{ v : v(\mathbf{x}) = \sum_{\ell=1}^{p_K} \alpha_\ell e^{ik \mathbf{d}_\ell \cdot (\mathbf{x} - \mathbf{x}_K)}, \alpha_\ell \in \mathbb{C} \right\}$$

where  $p_K$  is the number of *degrees of freedom* for the element  $K$ ,  $\mathbf{d}_\ell$ ,  $\ell = 1, \dots, p_K$  are  $p_K$  (roughly) **evenly spaced** unit direction vectors, and  $\mathbf{x}_K$  is the centre of the element.

Number of directions can be selected to give the same accuracy as a high-order polynomial DG method of order  $q$  with less degrees of freedom.

Basis Functions	2D	3D
DG ( $\mathcal{P}_q$ )	$(q+1)(q+2)/2$	$(q+1)(q+2)(q+3)/6$
DG ( $\mathcal{Q}_q$ )	$(q+1)^2$	$(q+1)^3$
Trefftz DG	$2q+1$	$(q+1)^2$

## Number of Degrees of Freedom

# Plane Waves

$$V_p(K) = \left\{ v : v(\mathbf{x}) = \sum_{\ell=1}^{p_K} \alpha_\ell e^{ik \mathbf{d}_\ell \cdot (\mathbf{x} - \mathbf{x}_K)}, \alpha_\ell \in \mathbb{C} \right\}$$

where  $p_K$  is the number of *degrees of freedom* for the element  $K$ ,  $\mathbf{d}_\ell$ ,  $\ell = 1, \dots, p_K$  are  $p_K$  (roughly) **evenly spaced** unit direction vectors, and  $\mathbf{x}_K$  is the centre of the element.

Number of directions can be selected to give the same accuracy as a high-order polynomial DG method of order  $q$  with less degrees of freedom.

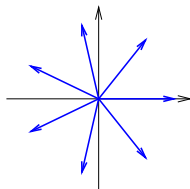
Basis Functions	2D	3D
DG ( $\mathcal{P}_q$ )	$(q+1)(q+2)/2$	$(q+1)(q+2)(q+3)/6$
DG ( $\mathcal{Q}_q$ )	$(q+1)^2$	$(q+1)^3$
Trefftz DG	$2q+1$	$(q+1)^2$

Number of Degrees of Freedom

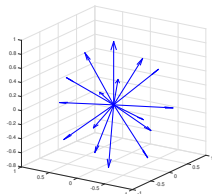
Direction Vectors

( $q = 3$ ):

2D



3D

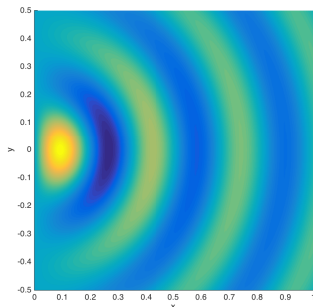


# TDG/DG FEM Comparison

Consider the smooth (analytic) solution (for [Acoustic Wave Propagation](#))

$$u(r, \theta) = \mathcal{J}_1(kr) \cos(\theta)$$

for  $k = 20$  on the domain  $\Omega = (0, 1) \times (-1/2, 1/2)$ .



Analytical Solution  
(Real Part)

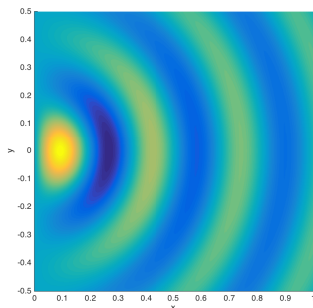
# TDG/DG FEM Comparison

Consider the smooth (analytic) solution (for **Acoustic Wave Propagation**)

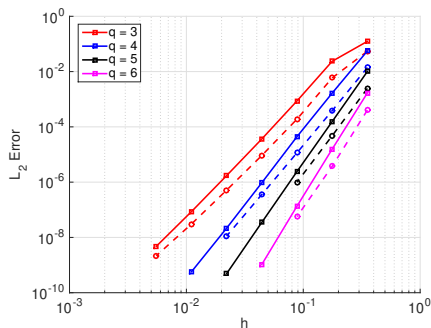
$$u(r, \theta) = \mathcal{J}_1(kr) \cos(\theta)$$

for  $k = 20$  on the domain  $\Omega = (0, 1) \times (-1/2, 1/2)$ .

We solve using both a DGFEM (solid line) and Trefftz DGFEM (dashed).



Analytical Solution  
(Real Part)



$\|u - u_{hp}\|_{L^2(\Omega)}$  vs.  $h$   
( $h$ -refinement)

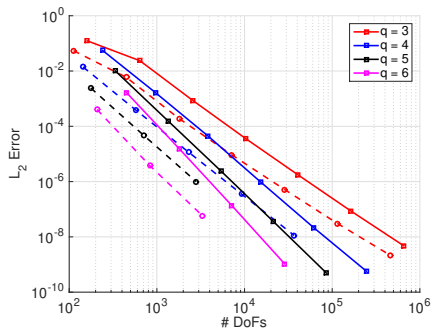
# TDG/DG FEM Comparison

Consider the smooth (analytic) solution (for [Acoustic Wave Propagation](#))

$$u(r, \theta) = \mathcal{J}_1(kr) \cos(\theta)$$

for  $k = 20$  on the domain  $\Omega = (0, 1) \times (-1/2, 1/2)$ .

We solve using both a DGFEM (solid line) and Trefftz DGFEM (dashed).



$\|u - u_{hp}\|_{L^2(\Omega)}$  vs. Degrees of Freedom  
( $h$ -refinement)

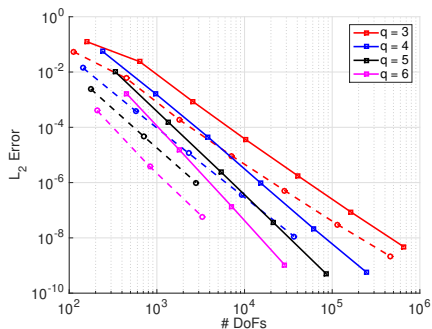
# TDG/DG FEM Comparison

Consider the smooth (analytic) solution (for [Acoustic Wave Propagation](#))

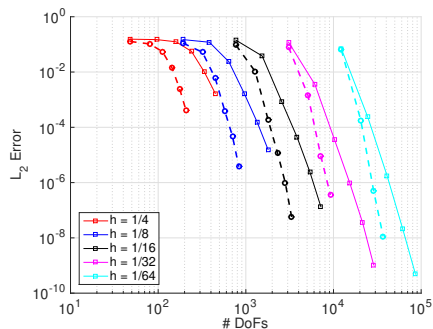
$$u(r, \theta) = \mathcal{J}_1(kr) \cos(\theta)$$

for  $k = 20$  on the domain  $\Omega = (0, 1) \times (-1/2, 1/2)$ .

We solve using both a DGFEM (solid line) and Trefftz DGFEM (dashed).



$\|u - u_{hp}\|_{L^2(\Omega)}$  vs. Degrees of Freedom  
( $h$ -refinement)



$\|u - u_{hp}\|_{L^2(\Omega)}$  vs. Degrees of Freedom  
( $p$ -refinement)

# TDG/DG FEM Comparison

Compared to standard DGFEM, plane wave-based Trefftz DGFEM has one major disadvantage:

For small mesh sizes, small wavenumbers, and high number of basis functions (plane wave directions) the basis functions are ill conditioned.

[Huttunen, Monk, Kaipio (2002); Luostari, Huttunen, Monk (2013)]

Compared to standard DGFEM, plane wave-based Trefftz DGFEM has one major disadvantage:

For small mesh sizes, small wavenumbers, and high number of basis functions (plane wave directions) the basis functions are ill conditioned.

[Huttunen, Monk, Kaipio (2002); Luostari, Huttunen, Monk (2013)]

It has been numerically shown that the condition number of the local mass matrix ( $M_K$ ) on an element behaves like

$$\text{cond}_2(M_K) \approx \frac{10^{p \ln p}}{(hk)^{p \ln(p/2.5)+7}};$$

although a modified Gram-Schmidt orthogonalization does improve the conditioning.

[C., Gedicke, Perugia (2017)]



# TDGFEM for Helmholtz

Given a mesh  $\mathcal{T}_h$  on  $\Omega$  we derive the TDGFEM as follows.

# TDFEM for Helmholtz

Given a mesh  $\mathcal{T}_h$  on  $\Omega$  we derive the TDFEM as follows.

- Multiply by test functions and integrate by parts, element-wise, **twice** (**ultra weak formulation**):

$$\int_K (-\Delta u - k^2 u) \bar{v} \, dx = 0$$

# TDGFEM for Helmholtz

Given a mesh  $\mathcal{T}_h$  on  $\Omega$  we derive the TDGFEM as follows.

- Multiply by test functions and integrate by parts, element-wise, **twice** (**ultra weak formulation**):

$$\int_K (\nabla u \cdot \nabla \bar{v} - k^2 u \bar{v}) dx - \int_{\partial K} \nabla u \cdot \mathbf{n}_K \bar{v} ds = 0$$

# TDGFEM for Helmholtz

Given a mesh  $\mathcal{T}_h$  on  $\Omega$  we derive the TDGFEM as follows.

- Multiply by test functions and integrate by parts, element-wise, **twice** (**ultra weak formulation**):

$$\int_K u(-\Delta \bar{v} - k^2 \bar{v}) \, dx + \int_{\partial K} u \nabla \bar{v} \cdot \mathbf{n}_K \, ds - \int_{\partial K} \nabla u \cdot \mathbf{n}_K \bar{v} \, ds = 0$$

# TDGFEM for Helmholtz

Given a mesh  $\mathcal{T}_h$  on  $\Omega$  we derive the TDGFEM as follows.

- Multiply by test functions and integrate by parts, element-wise, **twice** (**ultra weak formulation**):

$$\int_K u(-\Delta \bar{v} - k^2 \bar{v}) \, dx + \int_{\partial K} u \nabla \bar{v} \cdot \mathbf{n}_K \, ds - \int_{\partial K} \nabla u \cdot \mathbf{n}_K \bar{v} \, ds = 0$$

Given a mesh  $\mathcal{T}_h$  on  $\Omega$  we derive the TDGFEM as follows.

- Multiply by test functions and integrate by parts, element-wise, **twice** (**ultra weak formulation**):

$$\int_K u(-\Delta \bar{v} - k^2 \bar{v}) \, dx + \int_{\partial K} u \nabla \bar{v} \cdot \mathbf{n}_K \, ds - \int_{\partial K} \nabla u \cdot \mathbf{n}_K \bar{v} \, ds = 0$$

- Replace continuous functions by **discrete** approximations ( $u_{hp}, v_{hp} \in V_p(\mathcal{T}_h)$ ) and traces by **numerical fluxes**

$$u \rightarrow \hat{u}_{hp}, \quad \nabla u \rightarrow ik \hat{\sigma}_{hp}.$$

Given a mesh  $\mathcal{T}_h$  on  $\Omega$  we derive the TDGFEM as follows.

- Multiply by test functions and integrate by parts, element-wise, **twice** (**ultra weak formulation**):

$$\int_K u(-\Delta \bar{v} - k^2 \bar{v}) \, dx + \int_{\partial K} u \nabla \bar{v} \cdot \mathbf{n}_K \, ds - \int_{\partial K} \nabla u \cdot \mathbf{n}_K \bar{v} \, ds = 0$$

- Replace continuous functions by **discrete** approximations ( $u_{hp}, v_{hp} \in V_p(\mathcal{T}_h)$ ) and traces by **numerical fluxes**

$$u \rightarrow \hat{u}_{hp}, \quad \nabla u \rightarrow ik \hat{\sigma}_{hp}.$$

- $v \in V_p(\mathcal{T}_h) \subset T(\mathcal{T}_h) \implies -\Delta \bar{v} - k^2 \bar{v} = 0$  in  $K$ .

# TDGFEM for Helmholtz

Given a mesh  $\mathcal{T}_h$  on  $\Omega$  we derive the TDGFEM as follows.

- Multiply by test functions and integrate by parts, element-wise, **twice** (**ultra weak formulation**):

$$\int_K u(-\Delta \bar{v} - k^2 \bar{v}) \, dx + \int_{\partial K} u \nabla \bar{v} \cdot \mathbf{n}_K \, ds - \int_{\partial K} \nabla u \cdot \mathbf{n}_K \bar{v} \, ds = 0$$

- Replace continuous functions by **discrete** approximations ( $u_{hp}, v_{hp} \in V_p(\mathcal{T}_h)$ ) and traces by **numerical fluxes**

$$u \rightarrow \hat{u}_{hp}, \quad \nabla u \rightarrow ik \hat{\boldsymbol{\sigma}}_{hp}.$$

- $v \in V_p(\mathcal{T}_h) \subset T(\mathcal{T}_h) \implies -\Delta \bar{v} - k^2 \bar{v} = 0$  in  $K$ .

$$\int_{\partial K} \hat{u}_{hp} \nabla \bar{v}_{hp} \cdot \mathbf{n}_K \, ds - \int_{\partial K} ik \hat{\boldsymbol{\sigma}}_{hp} \cdot \mathbf{n}_K \bar{v}_{hp} \, ds = 0, \quad \text{for all } K \in \mathcal{T}_h.$$



# TDGFEM for Helmholtz

$$\begin{aligned}\{\{v\}\} &= \frac{v^+ + v^-}{2}, & \llbracket v \rrbracket &= v^+ \mathbf{n}^+ + v^- \mathbf{n}^-, & \forall \text{ scalar-valued functions } v. \\ \{\{\boldsymbol{\tau}\}\} &= \frac{\boldsymbol{\tau}^+ + \boldsymbol{\tau}^-}{2}, & \llbracket \boldsymbol{\tau} \rrbracket &= \boldsymbol{\tau}^+ \cdot \mathbf{n}^+ + \boldsymbol{\tau}^- \cdot \mathbf{n}^-, & \forall \text{ vector-valued functions } \boldsymbol{\tau}.\end{aligned}$$

$$\begin{aligned} \{\{v\}\} &= \frac{v^+ + v^-}{2}, & \llbracket v \rrbracket &= v^+ \mathbf{n}^+ + v^- \mathbf{n}^-, & \forall \text{ scalar-valued functions } v. \\ \{\{\boldsymbol{\tau}\}\} &= \frac{\boldsymbol{\tau}^+ + \boldsymbol{\tau}^-}{2}, & \llbracket \boldsymbol{\tau} \rrbracket &= \boldsymbol{\tau}^+ \cdot \mathbf{n}^+ + \boldsymbol{\tau}^- \cdot \mathbf{n}^-, & \forall \text{ vector-valued functions } \boldsymbol{\tau}. \end{aligned}$$

## Numerical Fluxes

$$ik\hat{\boldsymbol{\sigma}}_{hp} = \begin{cases} \{\{\nabla_h u_{hp}\}\} - \alpha ik \llbracket u_{hp} \rrbracket & \text{on interior faces,} \\ \nabla_h u_{hp} - (1 - \delta)(\nabla_h u_{hp} + ik\vartheta u_{hp} \mathbf{n} - \mathbf{g}_R \mathbf{n}) & \text{on faces on } \Gamma_R, \\ \nabla_h u_{hp} - \alpha ik u_{hp} \mathbf{n} & \text{on faces on } \Gamma_D, \end{cases}$$

$$\hat{u}_{hp} = \begin{cases} \{\{u_{hp}\}\} - \beta (ik)^{-1} \llbracket \nabla_h u_{hp} \rrbracket & \text{on interior faces,} \\ u_{hp} - \delta ((ik\vartheta)^{-1} \nabla_h u_{hp} \cdot \mathbf{n} + u_{hp} - (ik\vartheta)^{-1} \mathbf{g}_R) & \text{on faces on } \Gamma_R, \\ 0 & \text{on faces on } \Gamma_D, \end{cases}$$

with flux parameters  $\alpha, \beta, 0 < \delta \leq 1/2$ .

## Trefftz Discontinuous Galerkin FEM for Helmholtz

Find  $u_{hp} \in V_p(\mathcal{T}_h)$  such that,

$$\mathcal{A}_h(u_{hp}, v_{hp}) = \ell_h(v_{hp}),$$

for all  $v_{hp} \in V_p(\mathcal{T}_h)$ , where

$$\begin{aligned} \mathcal{A}_h(u, v) &= \int_{\mathcal{F}_h^I} \{u\} [\nabla_h \bar{v}] \, ds - \int_{\mathcal{F}_h^I} \beta(ik)^{-1} [\nabla_h u] [\nabla_h \bar{v}] \, ds \\ &\quad - \int_{\mathcal{F}_h^I \cup \mathcal{F}_h^D} \{\nabla_h u\} \cdot [\bar{v}] \, ds + \int_{\mathcal{F}_h^I \cup \mathcal{F}_h^D} \alpha ik [u] \cdot [\bar{v}] \, ds \\ &\quad + \int_{\mathcal{F}_h^R} (1 - \delta) u \nabla_h \bar{v} \cdot \mathbf{n} \, ds - \int_{\mathcal{F}_h^R} \delta (ik\vartheta)^{-1} (\nabla_h u \cdot \mathbf{n}) (\nabla_h \bar{v} \cdot \mathbf{n}) \, ds \\ &\quad - \int_{\mathcal{F}_h^R} \delta \nabla_h u \cdot \mathbf{n} \bar{v} \, ds + \int_{\mathcal{F}_h^R} (1 - \delta) ik\vartheta u \bar{v} \, ds, \\ \ell_h(v) &= - \int_{\mathcal{F}_h^R} \delta (ik\vartheta)^{-1} g_R \nabla_h \bar{v} \cdot \mathbf{n} \, ds + \int_{\mathcal{F}_h^R} (1 - \delta) g_R \bar{v} \, ds. \end{aligned}$$

Penalty Type	$\alpha$	$\beta$	$\delta$
<b>DG-type</b> Gittelsohn, Hiptmair & Perugia, 2009	$a q_K^2 / kh_K$	$b kh_K / q_K$	$dkh_K / q_K$
<b>Constant</b> Hiptmair, Moiola & Perugia, 2011	<b>a</b>	<b>b</b>	<b>d</b>
<b>UWVF</b> Cessenat & Després, 1998	$1/2$	$1/2$	$1/2$
<b>Non-Uniform Mesh</b> Hiptmair, Moiola & Perugia, 2014	$ah_{\max} / h_K$	$bh_{\max} / h_K$	$dh_{\max} / h_K$

## Section 3

# Adaptive Refinement

# Plane Wave Direction Refinement

Selecting plane wave directions which align with the wave direction of the analytical solution can reduce the error.

Several existing approaches exist for selecting plane wave directions:

- Ray-tracing — requires a source term. [Betcke & Phillips, 2012]
- Approximate

$$\frac{\nabla e(\mathbf{x}_0)}{ike(\mathbf{x}_0)},$$

where  $e$  is the error. [Gittelsohn, 2008 (Master's Thesis)]

- Adding an extra unknown (the optimal angle of rotation) to the basis functions. [Amara, Chaudhry, Diaz, Djellouli & Fiedler, 2014]

# Plane Wave Direction Refinement

Selecting plane wave directions which align with the wave direction of the analytical solution can reduce the error.

Several existing approaches exist for selecting plane wave directions:

- Ray-tracing — requires a source term. [Betcke & Phillips, 2012]
- Approximate

$$\frac{\nabla e(\mathbf{x}_0)}{ike(\mathbf{x}_0)},$$

where  $e$  is the error. [Gittelsohn, 2008 (Master's Thesis)]

- Adding an extra unknown (the optimal angle of rotation) to the basis functions. [Amara, Chaudhry, Diaz, Djellouli & Fiedler, 2014]

We propose using the Hessian of the numerical solution, based on work on anisotropic meshes for standard FE [Formaggia & Perotto, 2001, 2003].

# Plane Wave Direction Refinement

## Plane Wave Refinement Algorithm (2D)

Let  $(\lambda_1, \mathbf{v}_1), (\lambda_2, \mathbf{v}_2)$  be the eigenpairs of  $\mathbf{H}(\text{Re}(u_h(\mathbf{x}_K)))$ , and  $(\mu_1, \mathbf{w}_1), (\mu_2, \mathbf{w}_2)$  the eigenpairs of  $\mathbf{H}(\text{Im}(u_h(\mathbf{x}_K)))$  s.t.  $|\lambda_1| \geq |\lambda_2|$ ,  $|\mu_1| \geq |\mu_2|$ ; then, for constant  $C > 1$ , we can select the first plane wave direction as follows:

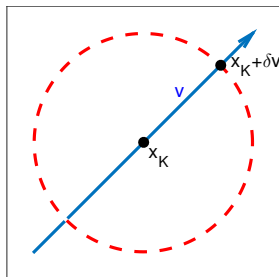
$ \lambda_1  \geq C \lambda_2 $	$ \mu_1  \geq C \mu_2 $	$ \lambda_1  \geq C \mu_1 $	$ \mu_1  \geq C \lambda_1 $	First PW
✓	✓	✓	✗	$\mathbf{v}_1$
✓	✓	✗	✓	$\mathbf{w}_1$
✓	✓	✗	✗	$\frac{(\mathbf{v}_1 + \mathbf{w}_1)}{\ \mathbf{v}_1 + \mathbf{w}_1\ }$
✓	✗	✓	✗	$\mathbf{v}_1$
✓	✗	✗	–	–
✗	✓	✗	✓	$\mathbf{w}_1$
✗	✓	–	✗	–
✗	✗	–	–	–

[C., Houston, Perugia (2018)]



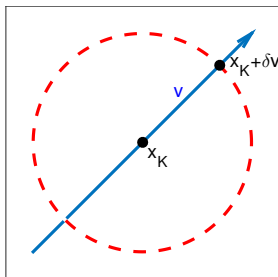
# Plane Wave Direction Refinement

If  $\mathbf{v}$  is the eigenvector, then the direction of propagation could be either  $\mathbf{v}$  or  $-\mathbf{v}$  (unknown orientation). Consider the impedance on the boundary of a ball (radius  $\delta$  around  $\mathbf{x}_K$ ) and compare to the plane wave  $u(\mathbf{x}) = e^{i\mathbf{k}\mathbf{d}\cdot(\mathbf{x}-\mathbf{x}_K)}$  for the cases when  $\mathbf{d} = \mathbf{v}$  and  $\mathbf{d} = -\mathbf{v}$ .



# Plane Wave Direction Refinement

If  $\mathbf{v}$  is the eigenvector, then the direction of propagation could be either  $\mathbf{v}$  or  $-\mathbf{v}$  (unknown orientation). Consider the impedance on the boundary of a ball (radius  $\delta$  around  $\mathbf{x}_K$ ) and compare to the plane wave  $u(\mathbf{x}) = e^{i\mathbf{k}\mathbf{d}\cdot(\mathbf{x}-\mathbf{x}_K)}$  for the cases when  $\mathbf{d} = \mathbf{v}$  and  $\mathbf{d} = -\mathbf{v}$ .

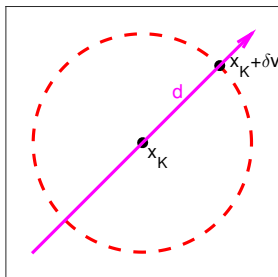


Evaluating at  $\mathbf{x}_K + \delta\mathbf{v}$  we note that the normal is  $\mathbf{v}$ , so we can calculate

$$\frac{\nabla u_h(\mathbf{x}_K + \delta\mathbf{v}) \cdot \mathbf{v} + iku_h(\mathbf{x}_K + \delta\mathbf{v})}{iku_h(\mathbf{x}_K + \delta\mathbf{v})}.$$

# Plane Wave Direction Refinement

If  $\mathbf{v}$  is the eigenvector, then the direction of propagation could be either  $\mathbf{v}$  or  $-\mathbf{v}$  (unknown orientation). Consider the impedance on the boundary of a ball (radius  $\delta$  around  $\mathbf{x}_K$ ) and compare to the plane wave  $u(\mathbf{x}) = e^{i\mathbf{k}\mathbf{d}\cdot(\mathbf{x}-\mathbf{x}_K)}$  for the cases when  $\mathbf{d} = \mathbf{v}$  and  $\mathbf{d} = -\mathbf{v}$ .



Evaluating at  $\mathbf{x}_K + \delta\mathbf{v}$  we note that the normal is  $\mathbf{v}$ , so we can calculate

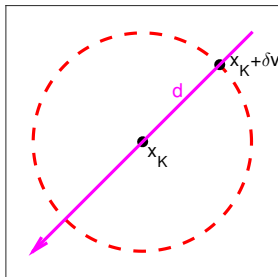
$$\frac{\nabla u_h(\mathbf{x}_K + \delta\mathbf{v}) \cdot \mathbf{v} + iku_h(\mathbf{x}_K + \delta\mathbf{v})}{iku_h(\mathbf{x}_K + \delta\mathbf{v})}.$$

We can compare this to the impedance for  $u$ :

$$\frac{\nabla u(\mathbf{x}_K + \delta\mathbf{v}) \cdot \mathbf{v}}{iku(\mathbf{x}_K + \delta\mathbf{v})} + 1 = \begin{cases} 2, & \text{if } \mathbf{d} = \mathbf{v}, \\ \end{cases}$$

# Plane Wave Direction Refinement

If  $\mathbf{v}$  is the eigenvector, then the direction of propagation could be either  $\mathbf{v}$  or  $-\mathbf{v}$  (unknown orientation). Consider the impedance on the boundary of a ball (radius  $\delta$  around  $\mathbf{x}_K$ ) and compare to the plane wave  $u(\mathbf{x}) = e^{i\mathbf{k}\mathbf{d}\cdot(\mathbf{x}-\mathbf{x}_K)}$  for the cases when  $\mathbf{d} = \mathbf{v}$  and  $\mathbf{d} = -\mathbf{v}$ .



Evaluating at  $\mathbf{x}_K + \delta\mathbf{v}$  we note that the normal is  $\mathbf{v}$ , so we can calculate

$$\frac{\nabla u_h(\mathbf{x}_K + \delta\mathbf{v}) \cdot \mathbf{v} + iku_h(\mathbf{x}_K + \delta\mathbf{v})}{iku_h(\mathbf{x}_K + \delta\mathbf{v})}.$$

We can compare this to the impedance for  $u$ :

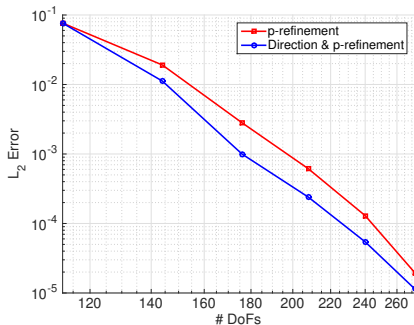
$$\frac{\nabla u(\mathbf{x}_K + \delta\mathbf{v}) \cdot \mathbf{v}}{iku(\mathbf{x}_K + \delta\mathbf{v})} + 1 = \begin{cases} 2, & \text{if } \mathbf{d} = \mathbf{v}, \\ 0, & \text{if } \mathbf{d} = -\mathbf{v}. \end{cases}$$

# Plane Wave Direction Refinement

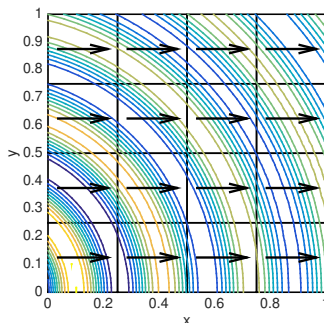
To test the direction refinement, we consider the solution

$$u(x, y) = \mathcal{H}_0^{(1)}(k\sqrt{(x + 0.25)^2 + y^2}),$$

with  $k = 20$ , on the domain  $\Omega = (0, 1)^2$ .



$\|u - u_{hp}\|_{L^2(\Omega)}$  vs. DoF



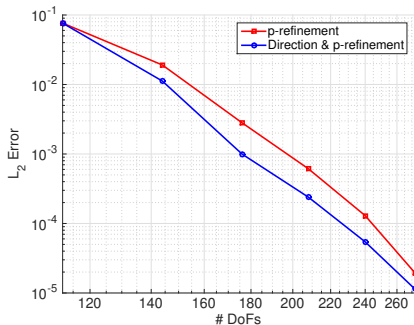
First PW Direction ( $p = 3$ )

# Plane Wave Direction Refinement

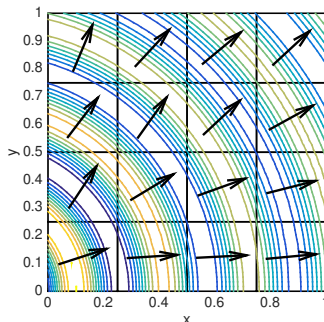
To test the direction refinement, we consider the solution

$$u(x, y) = \mathcal{H}_0^{(1)}(k\sqrt{(x + 0.25)^2 + y^2}),$$

with  $k = 20$ , on the domain  $\Omega = (0, 1)^2$ .



$\|u - u_{hp}\|_{L^2(\Omega)}$  vs. DoF



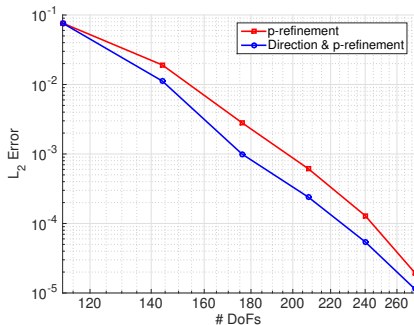
First PW Direction ( $p = 4$ )

# Plane Wave Direction Refinement

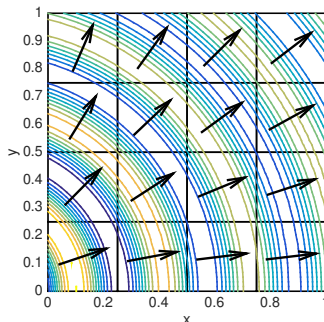
To test the direction refinement, we consider the solution

$$u(x, y) = \mathcal{H}_0^{(1)}(k\sqrt{(x + 0.25)^2 + y^2}),$$

with  $k = 20$ , on the domain  $\Omega = (0, 1)^2$ .



$\|u - u_{hp}\|_{L^2(\Omega)}$  vs.  $DoF$



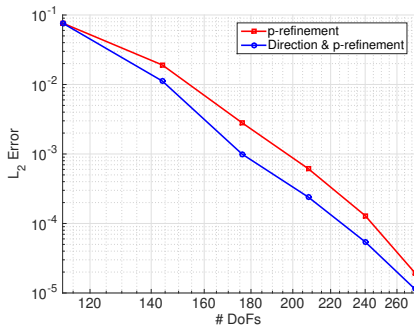
First PW Direction ( $p = 5$ )

# Plane Wave Direction Refinement

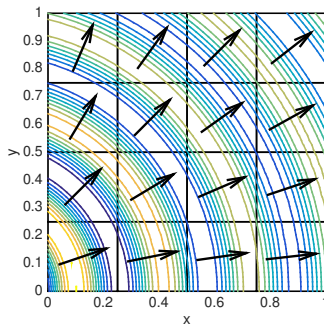
To test the direction refinement, we consider the solution

$$u(x, y) = \mathcal{H}_0^{(1)}(k\sqrt{(x + 0.25)^2 + y^2}),$$

with  $k = 20$ , on the domain  $\Omega = (0, 1)^2$ .



$\|u - u_{hp}\|_{L^2(\Omega)}$  vs.  $DoF$



First PW Direction ( $p = 6$ )

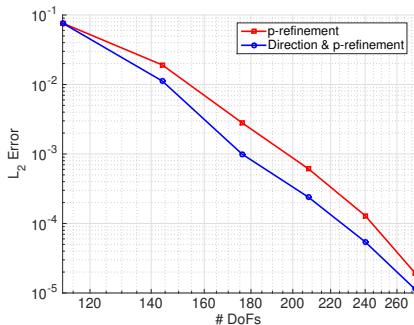


# Plane Wave Direction Refinement

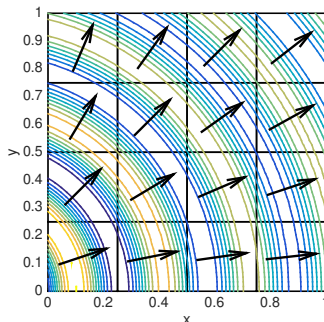
To test the direction refinement, we consider the solution

$$u(x, y) = \mathcal{H}_0^{(1)}(k\sqrt{(x + 0.25)^2 + y^2}),$$

with  $k = 20$ , on the domain  $\Omega = (0, 1)^2$ .



$\|u - u_{hp}\|_{L^2(\Omega)}$  vs. DoF



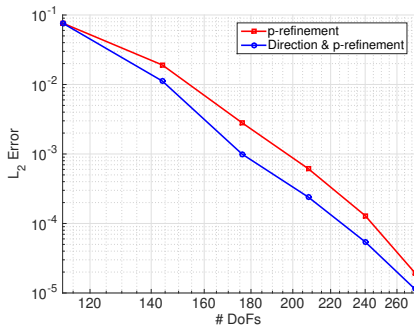
First PW Direction ( $p = 7$ )

# Plane Wave Direction Refinement

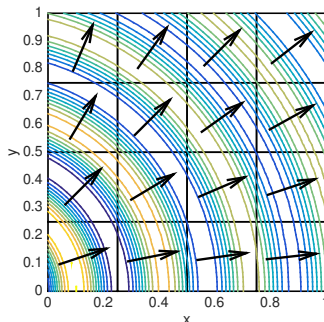
To test the direction refinement, we consider the solution

$$u(x, y) = \mathcal{H}_0^{(1)}(k\sqrt{(x + 0.25)^2 + y^2}),$$

with  $k = 20$ , on the domain  $\Omega = (0, 1)^2$ .



$\|u - u_{hp}\|_{L^2(\Omega)}$  vs. DoF



First PW Direction ( $p = 8$ )

An *a posteriori* error bounds exists for the  $h$ -version of the method in  $\mathbb{R}_2$ .

## *A posteriori* Error Bound — $h$ -version Only

For the TDGFEM, with the constant flux parameters, the following error bound holds:

$$\|u - u_h\|_{L^2(\Omega)}^2 \leq C(k, d_\Omega) \left\{ \left\| \alpha^{1/2} h_F^s \llbracket u_h \rrbracket \right\|_{L^2(\mathcal{F}_h^I \cup \mathcal{F}_h^D)}^2 + \frac{1}{k^2} \left\| \beta^{1/2} h_F^s \llbracket \nabla u_h \rrbracket \right\|_{L^2(\mathcal{F}_h^I)}^2 + \frac{1}{k^2} \left\| \delta^{1/2} h_F^s (g_R - \nabla u_h \cdot \mathbf{n}_F + ik\vartheta u_h) \right\|_{L^2(\mathcal{F}_h^R)}^2 \right\}$$

where  $s$  depends on the regularity of the solution to the adjoint problem ( $z \in H^{3/2+s}(\Omega)$ ).

[Kapita, Monk & Warburton, 2015]

## A *posteriori* Error Bound — hp-version

We propose the following potential *a posteriori* error bound with constants derived numerical to ensure the bound is efficient:

$$\|u - u_{hp}\|_{L^2(\Omega)}^2 \leq C \left\{ k \left\| \alpha^{1/2} h_F^{1/2} q_F^{-1/2} \llbracket u_{hp} \rrbracket \right\|_{L^2(\mathcal{F}_h^I \cup \mathcal{F}_h^D)}^2 \right. \\ \left. + \left\| \beta^{1/2} h_F^{3/2} q_F^{-3/2} \llbracket \nabla u_{hp} \rrbracket \right\|_{L^2(\mathcal{F}_h^I)}^2 \right. \\ \left. + \left\| \delta^{1/2} h_F^{3/2} q_F^{-3/2} (g_R - \nabla u_{hp} \cdot \mathbf{n}_F + iku_{hp}) \right\|_{L^2(\mathcal{F}_h^R)}^2 \right\}$$

for smooth solution of the adjoint.

[C., Houston, Perugia (2018)]

## Modified *hp*-refinement Strategy [Melenk & Wohlmuth, 2001]

Let  $\mathcal{T}_{h,0}$  be the initial mesh,  $\mathcal{T}_{h,i}$  the mesh after  $i$  refinements,  $\eta_{K,i}$  the error indicator for  $K \in \mathcal{T}_{h,i}$ , and  $\eta_{K,i}^{\text{pred}}$  the predicted error for  $K \in \mathcal{T}_{h,i}$ .

**for**  $K \in \mathcal{T}_{h,i}$  **do**

**if**  $K$  is marked for refinement **then**

**if**  $\eta_{K,i}^2 > (\eta_{K,i}^{\text{pred}})^2$  **then**

*h*-refinement: Subdivide  $K$  into  $N$  sons  $K_s, s \in 0, \dots, N$

$$(\eta_{K_s,i+1}^{\text{pred}})^2 \leftarrow \frac{1}{N} \gamma_h \left(\frac{1}{2}\right)^{2q_K} \eta_{K,i}^2, \quad i \leq s \leq N$$

**else**

*p*-refinement:  $q_K \leftarrow q_K + 1$

$$(\eta_{K,i+1}^{\text{pred}})^2 \leftarrow \gamma_p \eta_{K,i}^2$$

**end if**

**else**

$$(\eta_{K,i+1}^{\text{pred}})^2 \leftarrow \gamma_n (\eta_{K,i}^{\text{pred}})^2$$

**end if**

**end for**

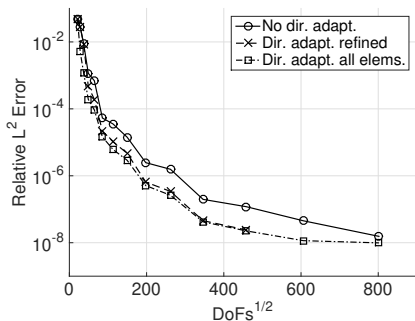
# Adaptive Refinement

Consider the smooth (analytic) solution (for [Acoustic Wave Propagation](#))

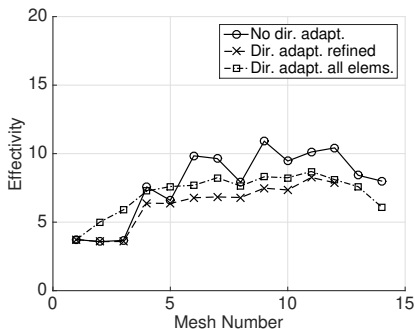
$$u(x, y) = \mathcal{H}_0^{(1)}(k\sqrt{(x + 1/4)^2 + y^2}),$$

on the domain  $\Omega = (0, 1)^2$  with suitable Robin BCs.

Consider  $h$ - and  $hp$ -refinement for  $k = 20$ .



$L^2$ -Error & Error Bound



Effectivity

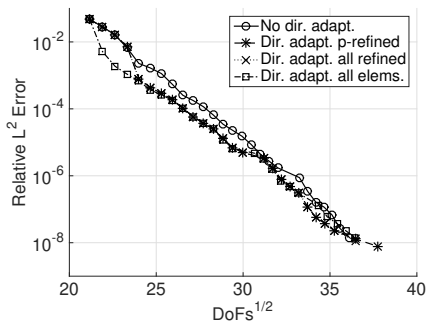
# Adaptive Refinement

Consider the smooth (analytic) solution (for [Acoustic Wave Propagation](#))

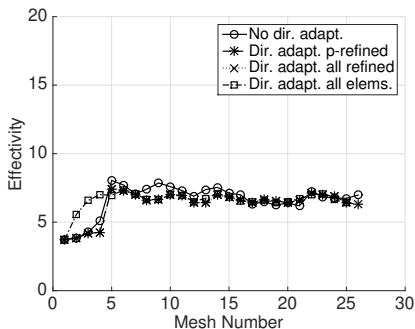
$$u(x, y) = \mathcal{H}_0^{(1)}(k\sqrt{(x + 1/4)^2 + y^2}),$$

on the domain  $\Omega = (0, 1)^2$  with suitable Robin BCs.

Consider  $h$ - and  $hp$ -refinement for  $k = 20$ .



$L^2$ -Error & Error Bound



Effectivity

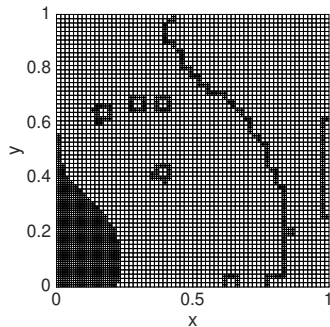
# Adaptive Refinement

Consider the smooth (analytic) solution (for [Acoustic Wave Propagation](#))

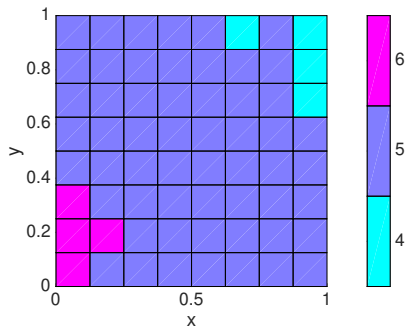
$$u(x, y) = \mathcal{H}_0^{(1)}(k\sqrt{(x + 1/4)^2 + y^2}),$$

on the domain  $\Omega = (0, 1)^2$  with suitable Robin BCs.

Consider  $h$ - and  $hp$ -refinement for  $k = 20$ .



Mesh after 8  $h$ -refinements



Mesh after 8  $hp$ -refinements



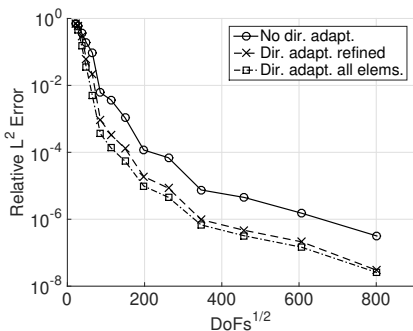
# Adaptive Refinement

Consider the smooth (analytic) solution (for [Acoustic Wave Propagation](#))

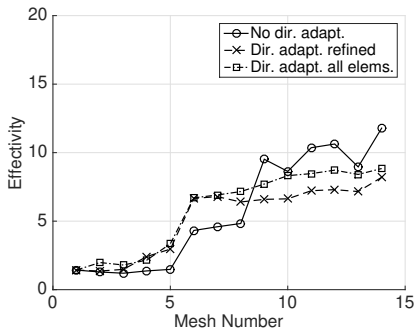
$$u(x, y) = \mathcal{H}_0^{(1)}(k\sqrt{(x + 1/4)^2 + y^2}),$$

on the domain  $\Omega = (0, 1)^2$  with suitable Robin BCs.

Consider  $h$ - and  $hp$ -refinement for  $k = 50$ .



$L^2$ -Error & Error Bound



Effectivity

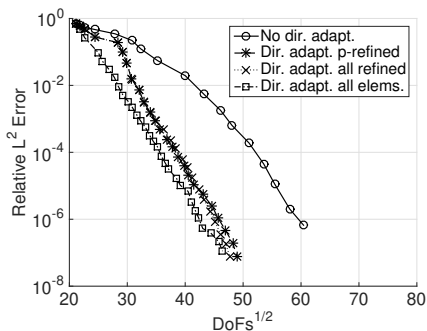
# Adaptive Refinement

Consider the smooth (analytic) solution (for [Acoustic Wave Propagation](#))

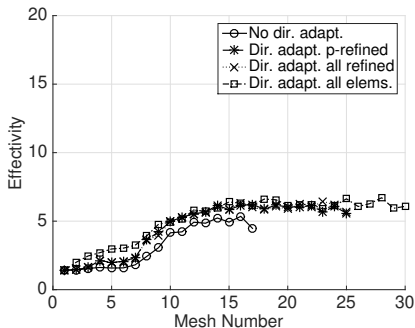
$$u(x, y) = \mathcal{H}_0^{(1)}(k\sqrt{(x + 1/4)^2 + y^2}),$$

on the domain  $\Omega = (0, 1)^2$  with suitable Robin BCs.

Consider  $h$ - and  $hp$ -refinement for  $k = 50$ .



$L^2$ -Error & Error Bound



Effectivity

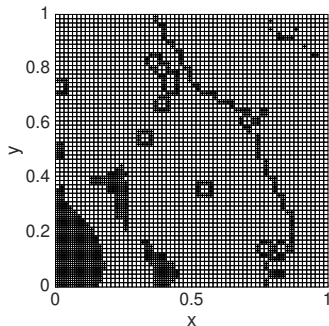
# Adaptive Refinement

Consider the smooth (analytic) solution (for [Acoustic Wave Propagation](#))

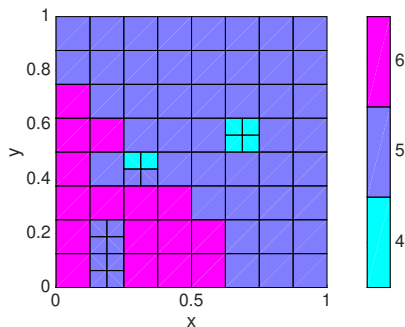
$$u(x, y) = \mathcal{H}_0^{(1)}(k\sqrt{(x + 1/4)^2 + y^2}),$$

on the domain  $\Omega = (0, 1)^2$  with suitable Robin BCs.

Consider  $h$ - and  $hp$ -refinement for  $k = 50$ .



Mesh after 8  $h$ -refinements



Mesh after 8  $hp$ -refinements

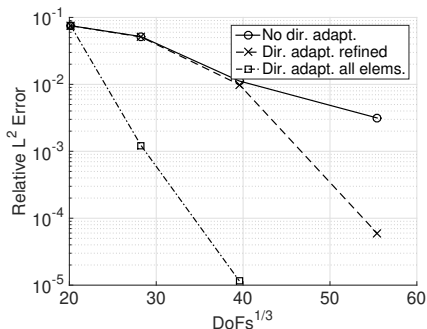
# Adaptive Refinement

Consider the 3D smooth (analytic) solution (for **Acoustic Wave Propagation**)

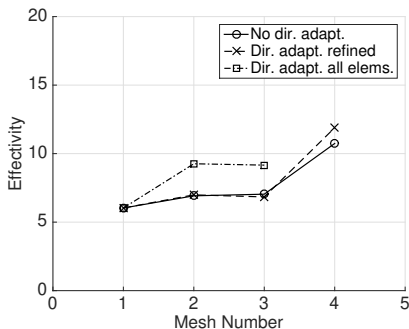
$$u(\mathbf{x}) = e^{i\mathbf{k}\cdot\mathbf{x}},$$

on the domain  $\Omega = (0, 1)^3$ , where  $\mathbf{d}_i = 1/\sqrt{3}$  for  $i = 1, 2, 3$ , with suitable Robin BCs.

Consider  $h$ - and  $hp$ -refinement for  $k = 20$ .



$L^2$ -Error & Error Bound



Effectivity

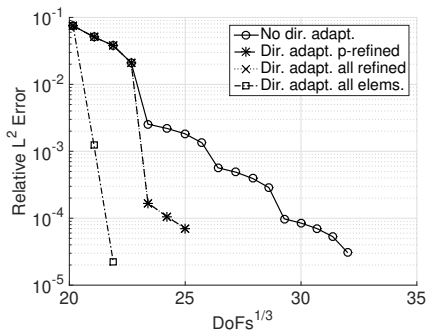
# Adaptive Refinement

Consider the 3D smooth (analytic) solution (for [Acoustic Wave Propagation](#))

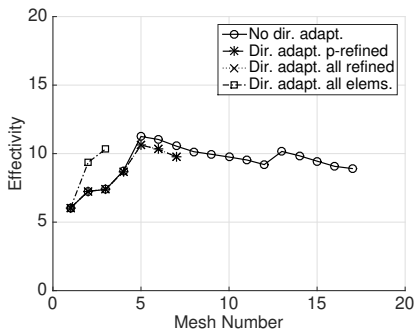
$$u(\mathbf{x}) = e^{i\mathbf{k}\cdot\mathbf{x}},$$

on the domain  $\Omega = (0, 1)^3$ , where  $\mathbf{d}_i = 1/\sqrt{3}$  for  $i = 1, 2, 3$ , with suitable Robin BCs.

Consider  $h$ - and  $hp$ -refinement for  $k = 20$ .



$L^2$ -Error & Error Bound



Effectivity

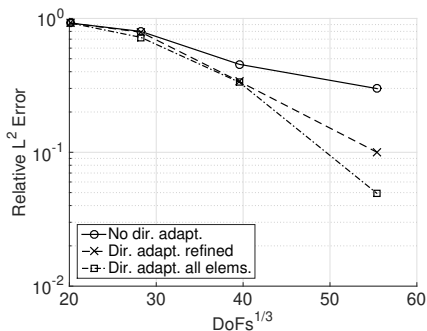
# Adaptive Refinement

Consider the 3D smooth (analytic) solution (for **Acoustic Wave Propagation**)

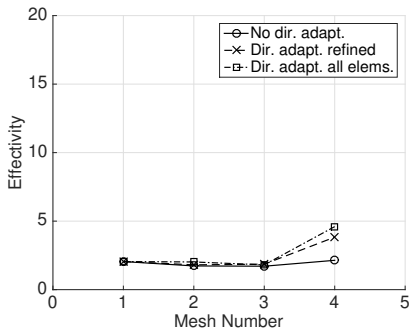
$$u(\mathbf{x}) = e^{i\mathbf{k}\cdot\mathbf{x}},$$

on the domain  $\Omega = (0, 1)^3$ , where  $\mathbf{d}_i = 1/\sqrt{3}$  for  $i = 1, 2, 3$ , with suitable Robin BCs.

Consider  $h$ - and  $hp$ -refinement for  $k = 50$ .



$L^2$ -Error & Error Bound



Effectivity

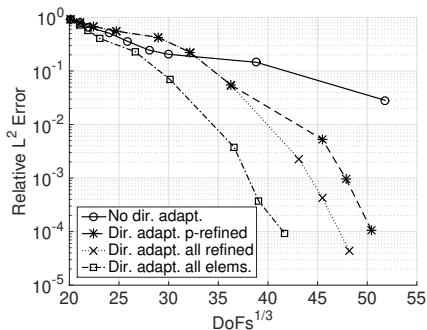
# Adaptive Refinement

Consider the 3D smooth (analytic) solution (for **Acoustic Wave Propagation**)

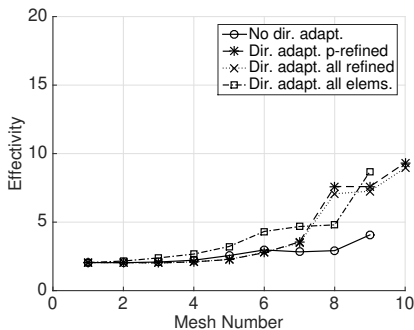
$$u(\mathbf{x}) = e^{i\mathbf{k}\cdot\mathbf{x}},$$

on the domain  $\Omega = (0, 1)^3$ , where  $\mathbf{d}_i = 1/\sqrt{3}$  for  $i = 1, 2, 3$ , with suitable Robin BCs.

Consider  $h$ - and  $hp$ -refinement for  $k = 50$ .



$L^2$ -Error & Error Bound



Effectivity

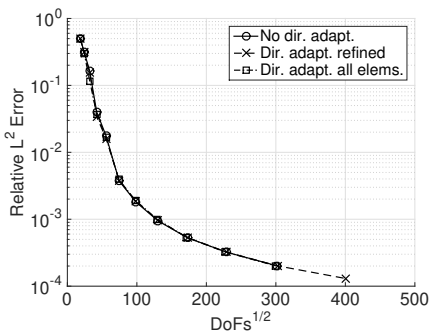
# Adaptive Refinement

Consider the non-smooth solution (for [Acoustic Wave Propagation](#))

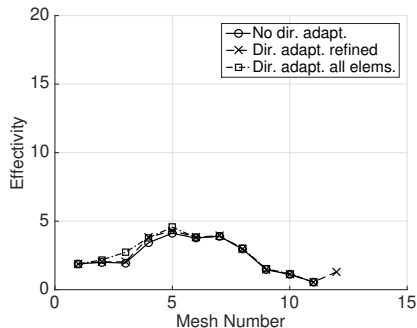
$$u(r, \theta) = \mathcal{J}_{2/3}(kr) \sin(2\theta/3),$$

on the domain L-shaped domain  $\Omega = (-1, 1)^2 \setminus (0, 1) \times (-1, 1)$ , with suitable Robin BCs.

Consider  $h$ - and  $hp$ -refinement for  $k = 20$ .



$L^2$ -Error & Error Bound



Effectivity



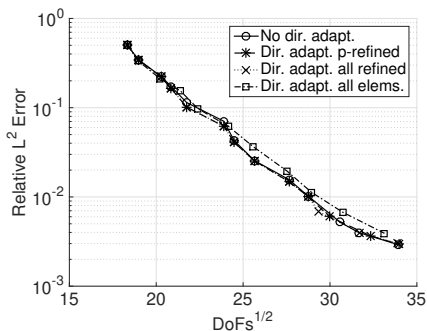
# Adaptive Refinement

Consider the non-smooth solution (for [Acoustic Wave Propagation](#))

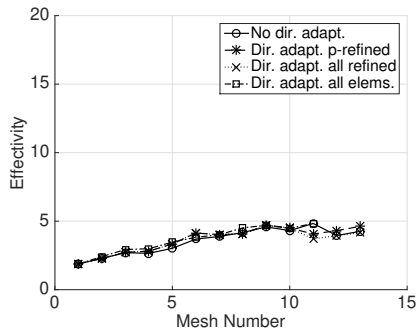
$$u(r, \theta) = \mathcal{J}_{2/3}(kr) \sin(2\theta/3),$$

on the domain L-shaped domain  $\Omega = (-1, 1)^2 \setminus (0, 1) \times (-1, 1)$ , with suitable Robin BCs.

Consider  $h$ - and  $hp$ -refinement for  $k = 20$ .



$L^2$ -Error & Error Bound



Effectivity

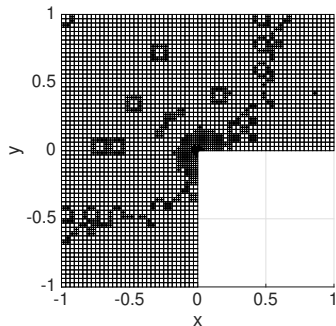
# Adaptive Refinement

Consider the non-smooth solution (for [Acoustic Wave Propagation](#))

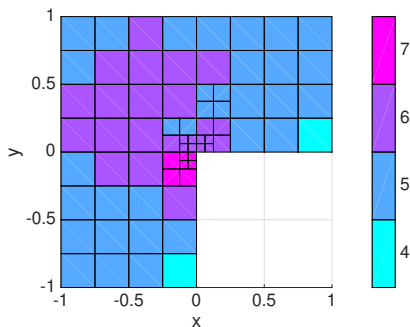
$$u(r, \theta) = \mathcal{J}_{2/3}(kr) \sin(2\theta/3),$$

on the domain L-shaped domain  $\Omega = (-1, 1)^2 \setminus (0, 1) \times (-1, 1)$ , with suitable Robin BCs.

Consider  $h$ - and  $hp$ -refinement for  $k = 20$ .



Mesh after 8  $h$ -refinements



Mesh after 8  $hp$ -refinements

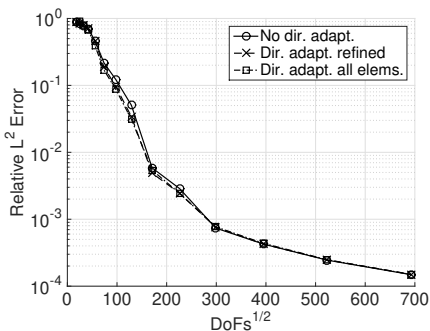
# Adaptive Refinement

Consider the non-smooth solution (for [Acoustic Wave Propagation](#))

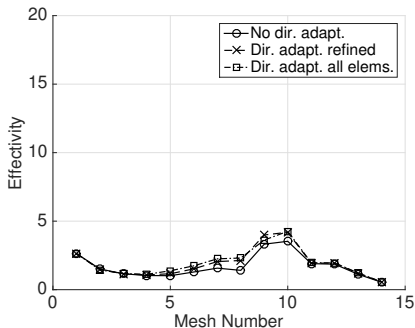
$$u(r, \theta) = \mathcal{J}_{2/3}(kr) \sin(2\theta/3),$$

on the domain L-shaped domain  $\Omega = (-1, 1)^2 \setminus (0, 1) \times (-1, 1)$ , with suitable Robin BCs.

Consider  $h$ - and  $hp$ -refinement for  $k = 50$ .



$L^2$ -Error & Error Bound



Effectivity

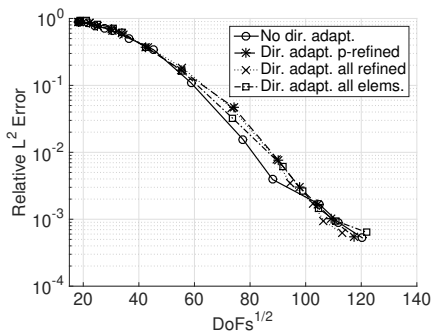
# Adaptive Refinement

Consider the non-smooth solution (for [Acoustic Wave Propagation](#))

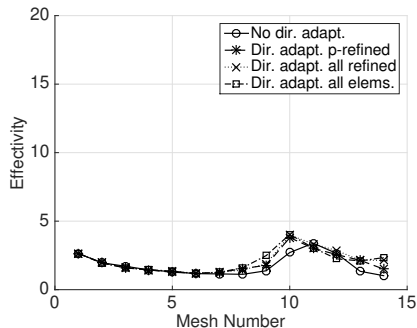
$$u(r, \theta) = \mathcal{J}_{2/3}(kr) \sin(2\theta/3),$$

on the domain L-shaped domain  $\Omega = (-1, 1)^2 \setminus (0, 1) \times (-1, 1)$ , with suitable Robin BCs.

Consider  $h$ - and  $hp$ -refinement for  $k = 50$ .



$L^2$ -Error & Error Bound



Effectivity

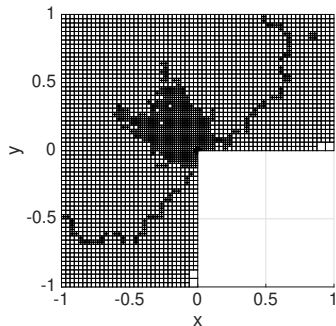
# Adaptive Refinement

Consider the non-smooth solution (for [Acoustic Wave Propagation](#))

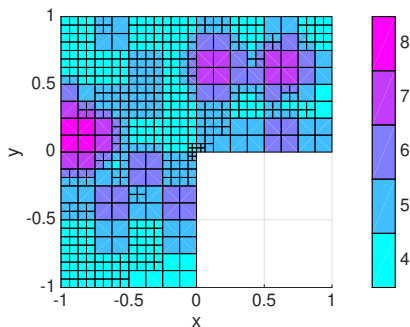
$$u(r, \theta) = \mathcal{J}_{2/3}(kr) \sin(2\theta/3),$$

on the domain L-shaped domain  $\Omega = (-1, 1)^2 \setminus (0, 1) \times (-1, 1)$ , with suitable Robin BCs.

Consider  $h$ - and  $hp$ -refinement for  $k = 50$ .



Mesh after 8  $h$ -refinements



Mesh after 8  $hp$ -refinements

# Adaptive Refinement

We now consider a wavenumber  $k$  given by the piecewise constant function

$$k(x, y) = \begin{cases} k_1 := \omega n_1 & \text{if } y \leq 0, \\ k_2 := \omega n_2 & \text{if } y > 0, \end{cases}$$

where, we  $\omega = 11$ ,  $n_1 = 2$ , and  $n_2 = 1$ , with appropriate inhomogeneous Dirichlet boundary condition, such that , for a constant  $0 \leq \theta_i \leq \pi/2$ ,

$$u(x, y) = \begin{cases} T e^{i(K_1 x + K_2 y)} & \text{if } y > 0, \\ e^{ik_1(x \cos(\theta_i) + y \sin(\theta_i))} + R e^{ik_1(x \cos(\theta_i) - y \sin(\theta_i))} & \text{if } y < 0, \end{cases}$$

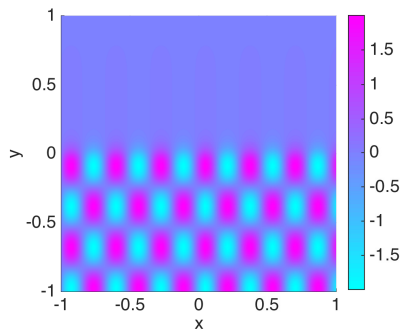
where  $K_1 = k_1 \cos(\theta_i)$ ,  $K_2 = \sqrt{k_2^2 - k_1^2 \cos^2(\theta_i)}$ ,

$$R = -\frac{K_2 - k_1 \sin(\theta_i)}{K_2 + k_1 \sin(\theta_i)},$$

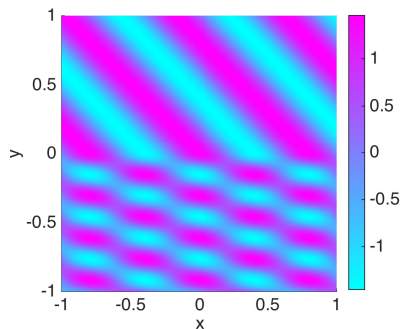
and  $T = 1 + R$ .

# Adaptive Refinement

There exists a critical angle  $\theta_{crit}$ , such that when  $\theta_i > \theta_{crit}$  the wave is refracted, while  $\theta_i < \theta_{crit}$  results in internal reflection.



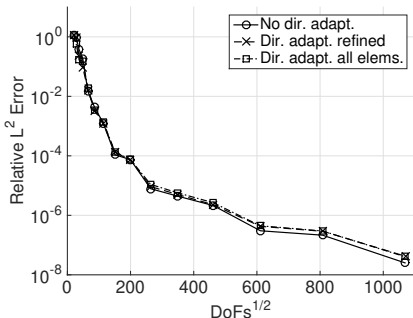
$\theta_i = 29^\circ$  — Analytical Soln.



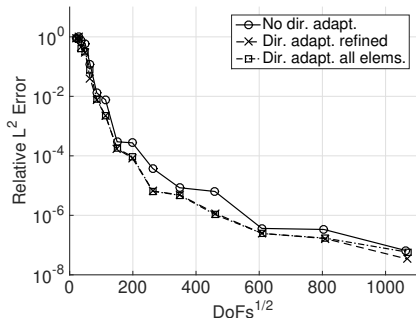
$\theta_i = 69^\circ$  — Analytical Soln.

# Adaptive Refinement

There exists a critical angle  $\theta_{crit}$ , such that when  $\theta_i > \theta_{crit}$  the wave is refracted, while  $\theta_i < \theta_{crit}$  results in internal reflection.



$\theta_i = 29^\circ$  —  $L^2$ -Error & Error Bound  
(h)

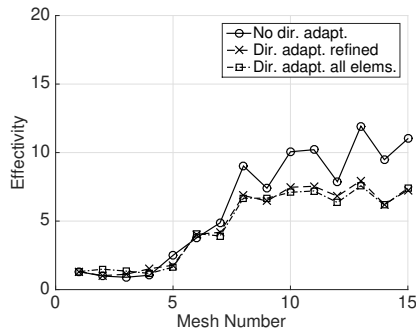


$\theta_i = 69^\circ$  —  $L^2$ -Error & Error Bound  
(h)

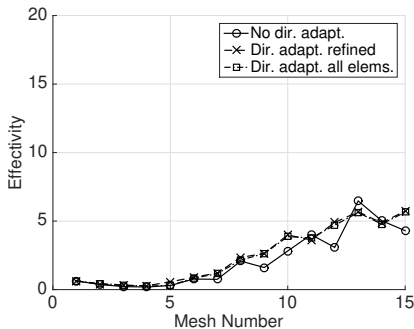


# Adaptive Refinement

There exists a critical angle  $\theta_{crit}$ , such that when  $\theta_i > \theta_{crit}$  the wave is refracted, while  $\theta_i < \theta_{crit}$  results in **internal reflection**.



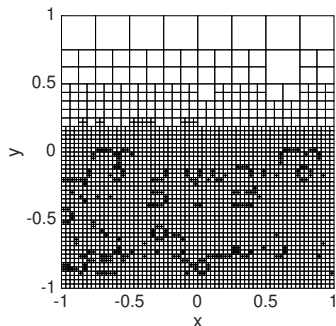
$\theta_i = 29^\circ$  — Effectivity ( $h$ )



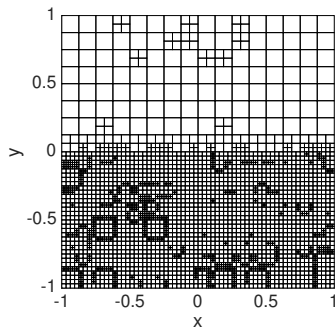
$\theta_i = 69^\circ$  — Effectivity ( $h$ )

# Adaptive Refinement

There exists a critical angle  $\theta_{crit}$ , such that when  $\theta_i > \theta_{crit}$  the wave is refracted, while  $\theta_i < \theta_{crit}$  results in internal reflection.



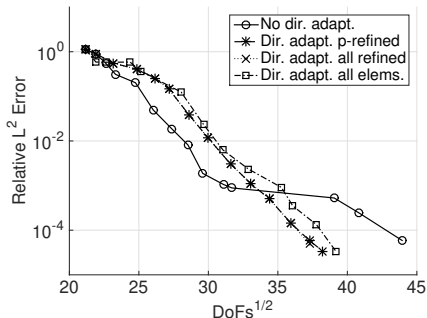
$\theta_i = 29^\circ$  — Mesh after 7  
*hp*-refinements



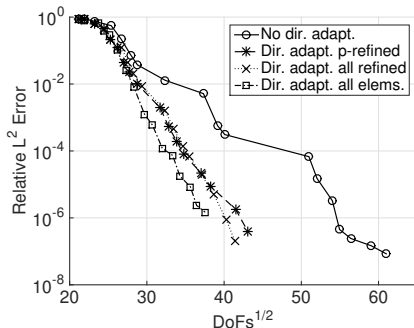
$\theta_i = 69^\circ$  — Mesh after 7  
*h*-refinements

# Adaptive Refinement

There exists a critical angle  $\theta_{crit}$ , such that when  $\theta_i > \theta_{crit}$  the wave is refracted, while  $\theta_i < \theta_{crit}$  results in internal reflection.



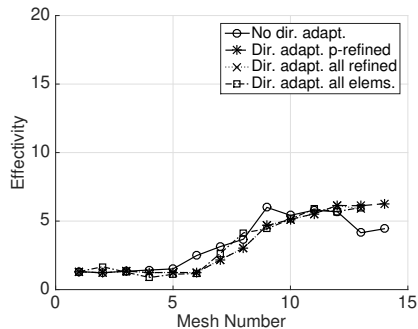
$\theta_i = 29^\circ$  —  $L^2$ -Error & Error Bound  
(hp)



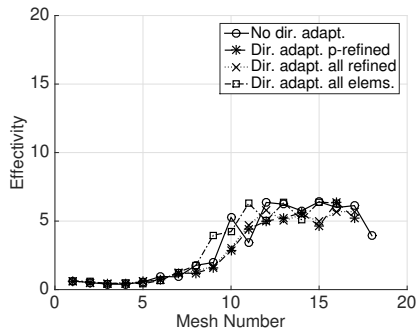
$\theta_i = 69^\circ$  —  $L^2$ -Error & Error Bound  
(hp)

# Adaptive Refinement

There exists a critical angle  $\theta_{crit}$ , such that when  $\theta_i > \theta_{crit}$  the wave is refracted, while  $\theta_i < \theta_{crit}$  results in **internal reflection**.



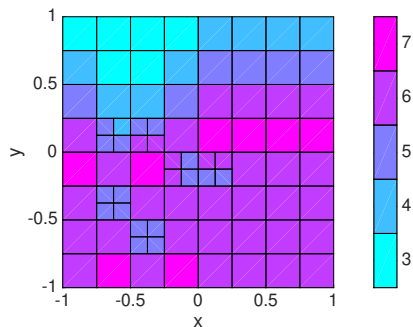
$\theta_i = 29^\circ$  — Effectivity (*hp*)



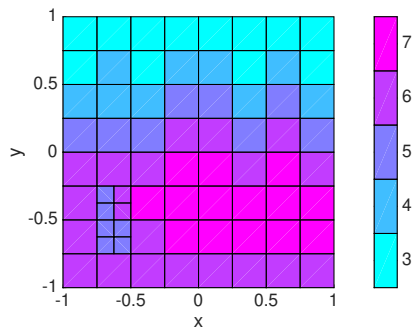
$\theta_i = 69^\circ$  — Effectivity (*hp*)

# Adaptive Refinement

There exists a critical angle  $\theta_{crit}$ , such that when  $\theta_i > \theta_{crit}$  the wave is refracted, while  $\theta_i < \theta_{crit}$  results in internal reflection.



$\theta_i = 29^\circ$  — Mesh after 7  
*hp*-refinements



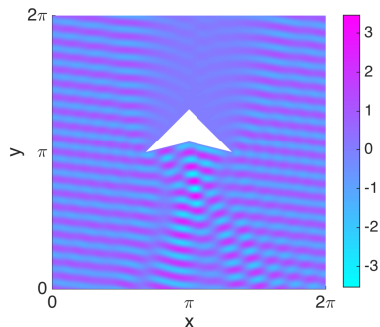
$\theta_i = 69^\circ$  — Mesh after 7  
*hp*-refinements

# Adaptive Refinement

Consider a scattering problem around an obstacle (kite). We impose homogeneous Dirichlet boundary conditions on the obstacle, and Robin boundary condition

$$g_R(\mathbf{x}) = \nabla u_I \cdot \mathbf{n} + iku_I, \quad u_I = e^{ik\mathbf{d}\cdot\mathbf{x}}$$

with  $k = 20$  and  $\mathbf{d} = -(\cos(6\pi/13), \sin(6\pi/13))^T$ .

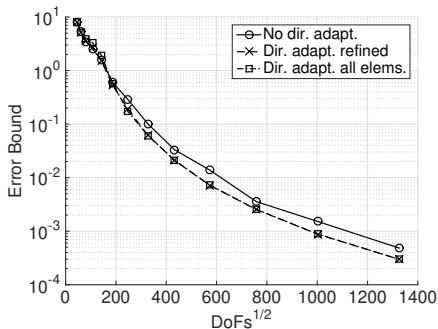


# Adaptive Refinement

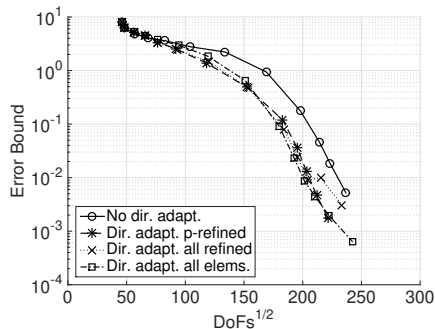
Consider a scattering problem around an obstacle (kite). We impose homogeneous Dirichlet boundary conditions on the obstacle, and Robin boundary condition

$$g_R(\mathbf{x}) = \nabla u_I \cdot \mathbf{n} + iku_I, \quad u_I = e^{ik\mathbf{d}\cdot\mathbf{x}}$$

with  $k = 20$  and  $\mathbf{d} = -(\cos(6\pi/13), \sin(6\pi/13))^T$ .



Error Bound (h)



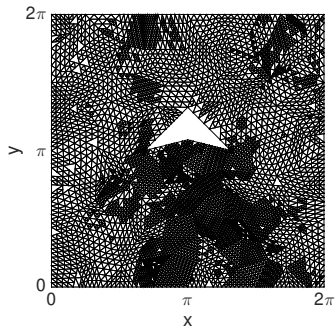
Error Bound (hp)

# Adaptive Refinement

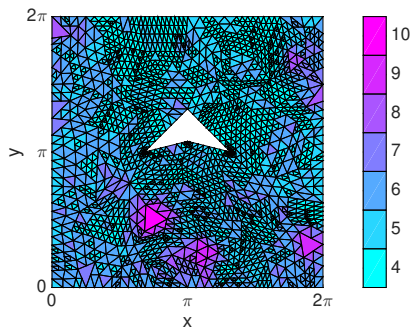
Consider a scattering problem around an obstacle (kite). We impose homogeneous Dirichlet boundary conditions on the obstacle, and Robin boundary condition

$$g_R(\mathbf{x}) = \nabla u_I \cdot \mathbf{n} + iku_I, \quad u_I = e^{i\mathbf{k}\mathbf{d}\cdot\mathbf{x}}$$

with  $k = 20$  and  $\mathbf{d} = -(\cos(6\pi/13), \sin(6\pi/13))^T$ .



Mesh after 9  $h$ -refinements



Mesh after 9  $hp$ -refinements

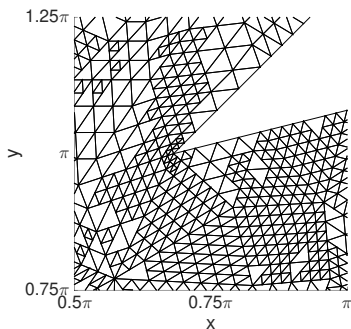


# Adaptive Refinement

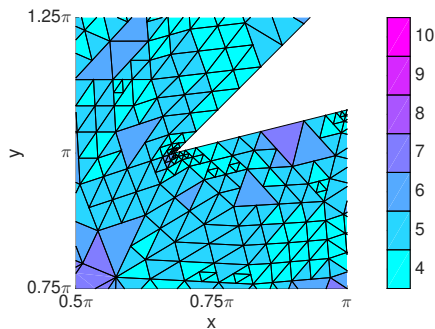
Consider a scattering problem around an obstacle (kite). We impose homogeneous Dirichlet boundary conditions on the obstacle, and Robin boundary condition

$$g_R(\mathbf{x}) = \nabla u_I \cdot \mathbf{n} + iku_I, \quad u_I = e^{i\mathbf{k}\cdot\mathbf{x}}$$

with  $k = 20$  and  $\mathbf{d} = -(\cos(6\pi/13), \sin(6\pi/13))^T$ .



Mesh after 9  $h$ -refinements



Mesh after 9  $hp$ -refinements

## Summary:

- With plane wave basis functions it is possible to refine the wave directions.
- $hp$ -adaptive refinement results in exponential convergence.
- Combining plane wave direction adaptivity with  $hp$ -adaptive refinement often leads to reduced error compared to standard refinement.

## Future Aims:

- Develop robust  $hp$ -version *a posteriori* error bounds..
- Use the eigenvalues/eigenvectors to develop **anisotropic**  $p$ -refinement (unevenly spaced plane waves).